ACSNANO

www.acsnano.org

ARTICLE

# Improved Lithium Ionic Conductivity in Composite Polymer Electrolytes with Oxide-Ion Conducting Nanowires

Wei Liu,[†] Dingchang Lin,[†] Jie Sun,[†] Guangmin Zhou,[†] and Yi Cui*[,†,‡]

[†]Department of Materials Science and Engineering, Stanford University, Stanford, California 94305, United States

[‡]Stanford Institute for Materials and Energy Sciences, SLAC National Accelerator Laboratory, 2575 Sand Hill Road, Menlo Park, California 94025, United States

Supporting Information

**ABSTRACT:** **Solid Li-ion electrolytes used in all-solid-state lithium-ion batteries (LIBs) are being considered to replace conventional liquid electrolytes that have leakage, flammability, and poor chemical stability issues, which represents one major challenge and opportunity for next-generation high-energy-density batteries. However, the low mobility of lithium ions in solid electrolytes limits their practical applications. Here, we report a solid composite polymer electrolyte with $Y_2O_3$-doped $ZrO_2$ (YSZ) nanowires that are enriched with positive-charged oxygen vacancies. The morphologies and ionic conductivities have been studied systemically according to concentration of $Y_2O_3$ dopant in the nanowires. In comparison to the conventional filler-free electrolyte with a conductivity of $3.62 \times 10^{-7}$ S cm$^{-1}$, the composite polymer electrolytes with the YSZ nanowires show much higher ionic conductivity. It indicates that incorporation of 7 mol % of $Y_2O_3$-doped $ZrO_2$ nanowires results in the highest ionic conductivity of $1.07 \times 10^{-5}$ S cm$^{-1}$ at 30 °C. This conductivity enhancement originates from the positive-charged oxygen vacancies on the surfaces of the nanowires that could associate with anions and then release more Li ions. Our work demonstrates a composite polymer electrolyte with oxygen-ion conductive nanowires that could address the challenges of all-solid-state LIBs.**

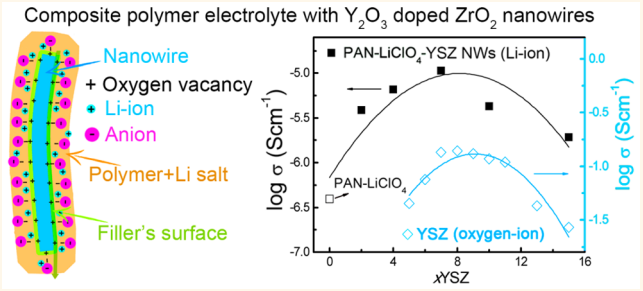


**KEYWORDS:** *composite polymer electrolyte, $Y_2O_3$-doped $ZrO_2$, nanowires, oxygen vacancy, Li-ion conduction*

Lithium-ion batteries (LIBs) have been intensively studied in order to meet the ever-growing demands of technologies ranging from portable devices, electric vehicles, to grid-scale energy storage. However, the current widely used liquid electrolyte with leakage, flammability, and poor chemical stability issues prevents the development of next-generation high-performance LIBs. By replacing the liquid electrolyte with a solid one that provides substantially improved safety and freedom design, the above problems can be resolved.[1−3] Furthermore, solid-state electrolytes could suppress the growth of lithium dendrites in lithium metal batteries. Lithium metal as the anode is the ultimate negative electrode that really takes advantage of the high specific capacity of cathodes (*e.g.*, sulfur).[4−7] Additional, solid electrolytes can also be adopted in liquid batteries to suppress unwanted redox shuttles.[8−10] However, using solid Li-ion electrolytes results in decreased capacity utilization and performance deterioration due to the low ionic conductivity and high interfacial resistance in contact with electrodes, which remains the principle design challenge.

Currently, solid Li-ion electrolytes can be divided into two general types: inorganic materials and organic polymers. A large number of inorganic oxide electrolytes have been investigated widely, such as the garnet oxides $Li_xLa_3M_2O_{12}$ (M = Ta, Nb, Zr),[11] NASICON (sodium super ionic conductor)-type phosphates,[12] perovskite-type $Li_{3x}La_{2/3-x1/3-2x}TiO_3$.[13] However, the ionic conductivity of these oxides up to $1.0 \times 10^{-4}$ S cm$^{-1}$ at room temperature (RT) is still not sufficiently high to satisfy demand. Recently, $Li_{10}GeP_2S_{12}$[14] with an unprecedented conductivity of $1.2 \times 10^{-2}$ S cm$^{-1}$ and $Li_2S-P_2S_5$[15] glass ceramics of $3.2 \times 10^{-3}$ S cm$^{-1}$ have been reported. However, these sulfides are either unstable with Li metal and with high voltage cathode materials or extremely hydroscopic, producing toxic $H_2S$ in contact with moisture. In addition, the fabrication process of the ceramic electrolyte is also difficult. Compared with inorganic electrolytes, solid polymer electrolytes (SPEs)

Received: October 9, 2016
Accepted: November 22, 2016
Published: November 22, 2016




DOI: 10.1021/acsnano.6b06797
*ACS Nano* 2016, 10, 11407−11413

present more structure flexibility as well as easier lamination stacking and hermetic sealing processes to meet the requirements of different cell applications, to which much attention sustained over the past few decades has been devoted. However, widely studied SPEs based on poly(ethylene oxide) (PEO) or polyacrylonitrile (PAN) usually show a low ionic conductivity of $10^{-7}$ S $cm^{-1}$ at RT.[16] Therefore, due to their low ionic conductivity and poor mechanical property, SPEs have not, so far, been widely commercialized.[17−21] To address these concerns, dispersing ceramic nanoparticles including $SiO_2$, $TiO_2$, $Al_2O_3$, $ZrO_2$, $Sm_2O_3$, and $LiAlO_2$ that provide competitive interactions within the polymer matrix is an effective approach, which increases ionic conductivity and, meanwhile, improves electrochemical stability and mechanical properties. Studies have shown that $Li^+$ transport is coupled with segmental motion of the polymer chain in SPEs. The addition of nanoparticles is believed to hinder local reorganization of chains in the polymer and decrease the polymer crystallization, which favors high Li-ion transport. Meanwhile, a large number of investigations indicated that Lewis acid−base model interaction also soundly supports the increased ionic conductivity, which is an interesting area and approach to improve electrochemical performance of composite polymer electrolytes.[22−30]

It is well-recognized that the Lewis acid sites enriched on the filler surfaces can interact strongly with anions of salt, set free the positively charged Li ions, and subsequently improve ionic conductivity of the composite polymer electrolyte.[5,20,27,30−33] Oxygen-ion conducting ceramics developed for solid oxide fuel cells (SOFCs) and sensors could offer such an opportunity, which have not been considered before. It is widely acknowledged, due to its high ionic conductivity coupled with chemical, thermodynamic, and mechanical stability over a wide temperature and oxygen partial pressure range, $Y_2O_3$-doped $ZrO_2$ (YSZ) is regarded as one of the most reliable oxide-ion conductors at high temperatures.[34−39] The metal ion dopants with a low oxidation state can create high concentration of oxygen vacancies in $ZrO_2$. The oxygen vacancies in YSZ are positively charged and can serve as Lewis acid sites in the composite polymer electrolyte, as shown in Figure 1. Here, we demonstrated that oxygen-ion conducting YSZ nanowires could effectively enhance the ionic conductivity of the PAN−$LiClO_4$ polymer electrolyte. Moreover, the reason to use nanowires instead of nanoparticles is that our previous study[19] demonstrated that the nanowires could offer a more continuous ion conducting pathway across much longer distance and generate effective percolation network, rather than nanoparticles that are isolated (Figure 1). Also, it should be noted that YSZ shows very low ionic conductivity at RT, whose own ionic conductivity contribution is negligible in the composite polymer electrolyte.

## RESULTS AND DISCUSSION

The synthesis procedure of SPEs with YSZ nanowires is illustrated in Figure S1. YSZ nanowires with various concentrations of dopants and diameters could be successfully prepared by electrospining and following calcination. SPEs were obtained by casting with the solution of PAN, $LiClO_4$, and the YSZ nanowires in dimethylformamide (DMF) solvent and then by drying in high vacuum at 80 °C to completely remove the solvent. Figure 2 displays the X-ray diffraction (XRD) patterns at RT for the YSZ nanowires with variable Y doping concentrations, which provides deep insights into the phase

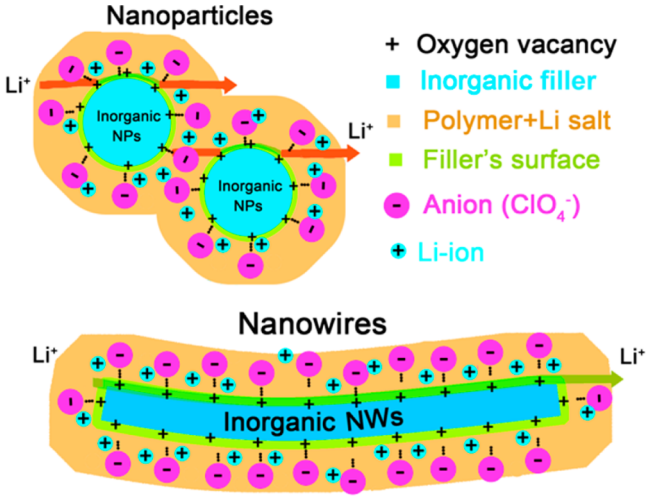


**Figure 1. Schematic illustration for Li-ion transport in the composite polymer electrolytes with nanoparticle and nanowire fillers. The positive-charged oxygen vacancies on the surfaces of the fillers act as Lewis acid sites that can interact strongly with anions and release Li ions. A continuous fast conduction pathway can be seen for nanowires rather than nanoparticles.**

stabilization. It can be seen from high-resolution XRD patterns in Figure 2b,c that the peaks of pure $ZrO_2$ without dopant show no evidence corresponding to the monoclinic structure, which indicates that the high-temperature phase of the tetragonal phase can be stabilized at RT in the $ZrO_2$ nanowires. It is well-known that the splitting between (004) and (400) peaks around 72−76° is associated with the tetragonal phase.[40] This peak splitting disappears when doping level reaches 4 mol %, implying that the dominated phase in the 4YSZ nanowires is the cubic phase. It clearly shows that in comparison to the traditional course-grained YSZ materials, the high-temperature phases of tetragonal and cubic could be stabilized at RT with lower $Y_2O_3$ doping concentrations, due to a nanosize effect. It is reported that high-temperature phases could be stabilized in nanocrystalline materials when the grain size is smaller than the critical crystallite size, which is primarily due to increased surface energy.[27,31−33] The critical sizes are about 10−50 and 5−10 nm for $ZrO_2$ without dopants, below which the tetragonal and cubic phases can be stabilized at RT, respectively.[41,42] Figure S2 shows the X-ray photoemission spectroscopy (XPS) of the YSZ nanowires with various concentrations of dopants. The molar ratios of Y/Zr calculated from theoretical compositions and measured from XPS spectra are listed in Table S1, which indicates that the surface composition is nearly the same as the theoretical stoichiometry for the YSZ nanowires.

Identical morphological features of the calcined 7 mol % of $Y_2O_3$-doped $ZrO_2$ (7YSZ) nanowires with large aspect ratios can be observed in transmission electron microscopy (TEM) images (Figure 3a,b), showing high aspect ratio and smooth surfaces. The inset figure in Figure 3b illustrates the diameter distributions of the 7YSZ nanowires, showing an average diameter of 55 nm. Figure 3c displays the high-resolution TEM (HRTEM) image, indicating the cubic phase and excellent crystallinity in the nanowires. Together with the corresponding selected area electron diffraction (SAED) pattern in the inset of Figure 3c shows a polycrystalline structure that can be indexed in a cubic cell, which is in agreement with the XRD pattern results. As shown Figure 3c, the grain size of the nanowires is


DOI: 10.1021/acsnano.6b06797
ACS Nano 2016, 10, 11407−11413

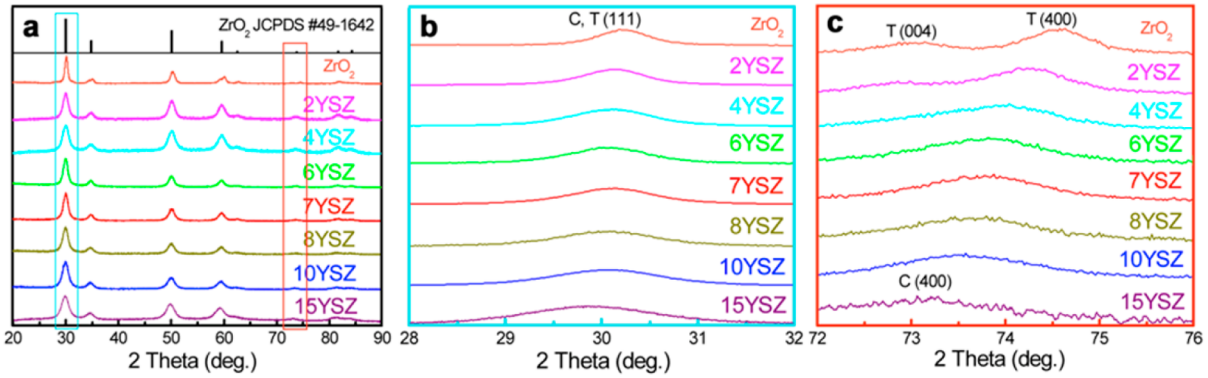


**Figure 2. XRD patterns of the YSZ nanowires with various $Y_2O_3$ doping levels. XRD patterns taken at (a) 20−90°. High-resolution XRD patterns at (b) 28−32 and (c) 72−76°.**

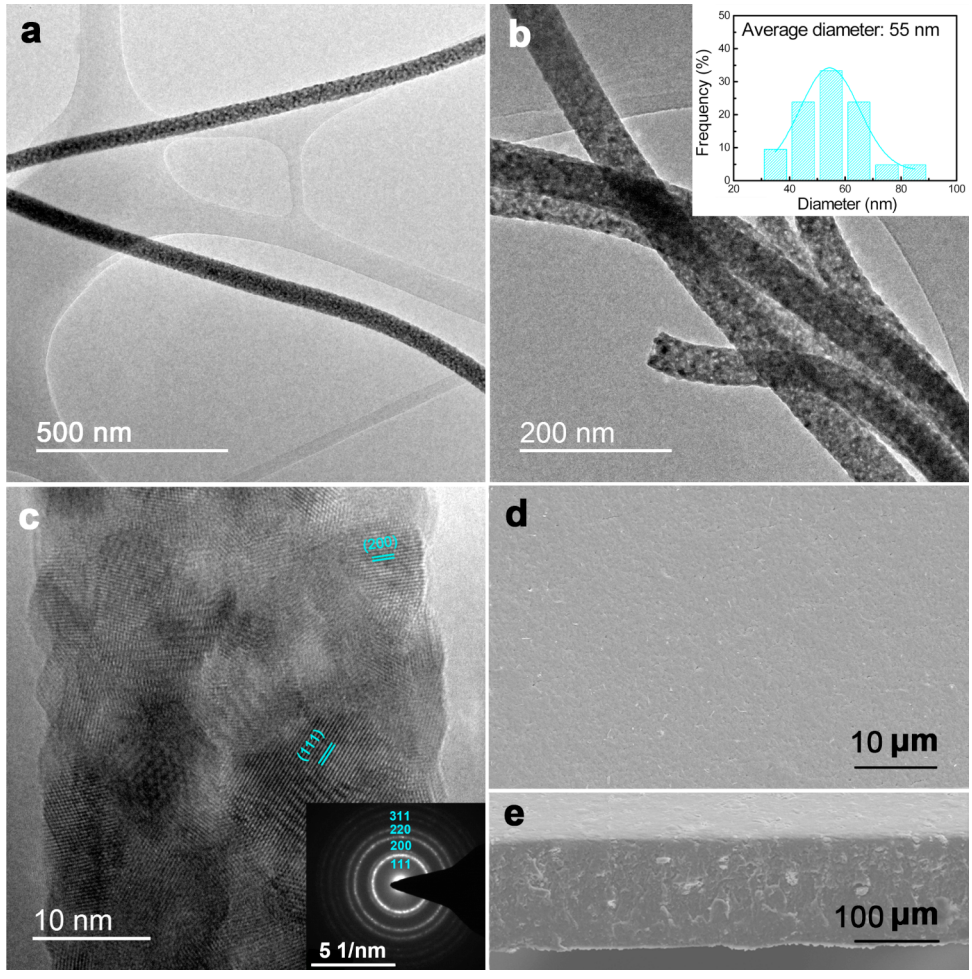


**Figure 3. Morphologies of the YSZ nanowires. (a,b) TEM images of the nanowires. The inset in (b) is diameter distributions of the nanowires. (c) HRTEM image of the nanowire, with corresponding SAED pattern. (d) SEM image of the composite polymer electrolyte with YSZ nanowires, together with the (e) cross-sectional SEM image.**

only around 10 nm, which is within the range of the critical sizes for stabilizing tetragonal phases in the undoped $ZrO_2$. Hence, the high-temperature phases of tetragonal and cubic could be stabilized at lower Y doping concentrations. Figure S3 further shows more TEM images of the YSZ nanowires with various concentrations of dopants synthesized using two kinds of solvents for the precursors, including the mixture solvent of deionized water and ethanol (wt ratio is 4:6) (Figure S3a−d), and the pure solvent of ethanol (Figure S3e−h). Figure 3d,e displays the top view and cross-sectional scanning electron microscopy (SEM) images of the composite polymer electrolyte with 15 wt % 7YSZ nanowires (diameter is 55 nm), which indicates that the composite electrolyte film is smooth and the YSZ nanowires are uniformly distributed and fully embedded in the PAN matrix.

The electrical properties of the composite polymer electrolytes were studied in the following study. The typical AC impedance spectra with well-fitted spectra for the composite



DOI: 10.1021/acsnano.6b06797
ACS Nano 2016, 10, 11407−11413

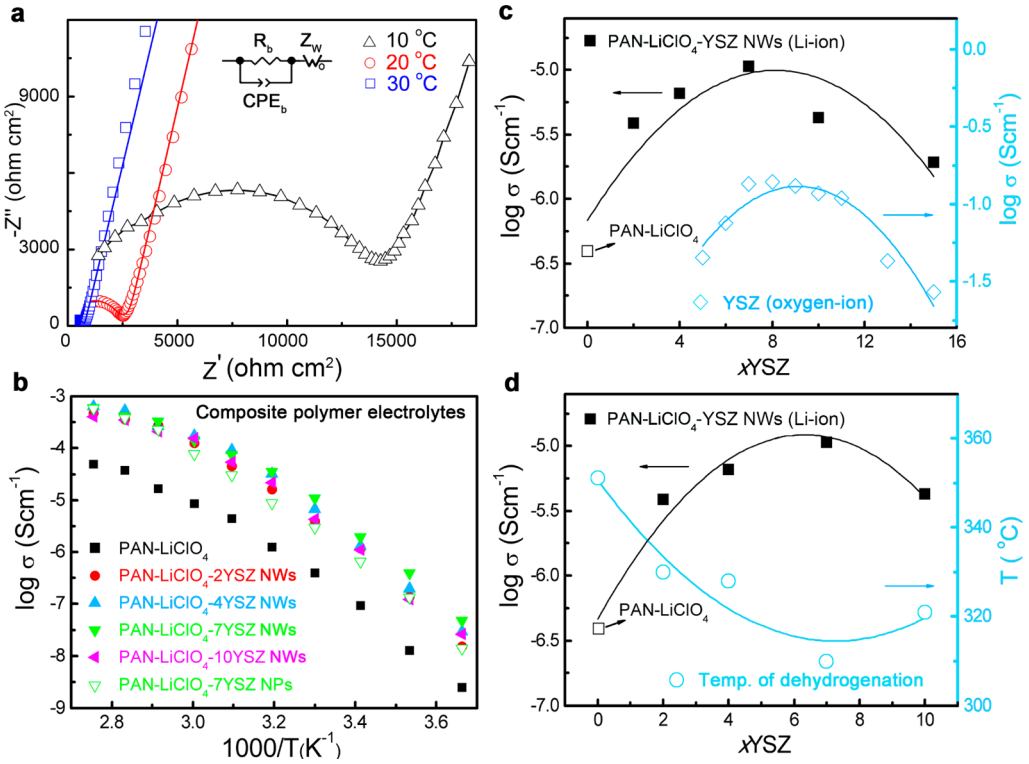


**Figure 4. Electrical properties of the composite polymer electrolyte filled with the YSZ nanowires. (a) Experimental and fitting impedance spectra for the composite electrolyte with YSZ nanowires at different measuring temperatures and equivalent circuit. (b) Arrhenius plots of the composite electrolytes with the YSZ nanowires with 55 nm diameter of various doping concentrations. (c) Relationship between the Y doping level and the conductivity, together with the conductivity of the YSZ bulk (data of the YSZ bulk conductivity are from ref 37). (d) Plots of ionic conductivity and temperature of dehydrogenation *vs* $Y_2O_3$ doping level.**

polymer electrolytes with YSZ nanowires measured at various temperatures are given in Figure 4a. A well-defined semicircle at high and intermediate frequencies ascribed to the bulk resistance and a spike at low frequencies corresponding to the double-layer capacitance formed at the interface between electrode and electrolyte can be observed. The equivalent circuit shown in the inset is used to fit these spectra, where $R_b$ is the bulk resistance of the polymer electrolytes, $CPE_b$ is the constant-phase element to fit bulk capacitance, and $Z_w$ is Warburg impedance due to an ion-diffusion-limited process. CPE is used to model the slightly depressed nature of the semicircle arcs rather than capacitors. The ionic conductivity $\sigma$ for the solid electrolytes can be then converted from a resistance $R$ data measured *via* impedance spectra measurements at different temperatures, as shown in the following equation:

$$\sigma = \frac{1}{R}\frac{L}{S} \quad (1)$$

where $L$ is the membrane thickness and $S$ is the effective electrode area.

The Arrhenius plots for the composite polymer electrolytes with the YSZ nanowires of 55 nm diameter, with YSZ nanoparticles and filler-free electrolyte, are shown in Figure 4b. Compared with the filler-free electrolyte ($3.62 \times 10^{-7}$ S cm$^{-1}$), the composite polymer electrolyte with 7YSZ nanoparticles shows a higher ionic conductivity of $2.98 \times 10^{-6}$ S cm$^{-1}$ at 30 °C. It should be noted that the oxygen-ion conductivity of the YSZ fillers could be ignored at RT. Therefore, the oxygen-ion conductive filler therefore is shown to have an effect on increasing Li-ion conductivity of the composite polymer electrolyte. It also can be seen that the conductivity can be further enhanced to $1.07 \times 10^{-5}$ S cm$^{-1}$ (7YSZ) by the addition of YSZ nanowires. That supports the mechanism of more continuous fast ion conduction pathway being formed by nanowires than nanoparticles. In addition, the composite polymer electrolyte also demonstrates increased electrochemical stability, as shown in Figures S4 and S5. The peak observed below 0 V and the peak around 0.2 V are attributed to lithium plating and stripping.[1] Herein, the composite polymer electrolyte with the YSZ nanowires is a promising candidate of inorganic fillers, used in all-solid-state LIBs for the application. Compared with reported composite polymer electrolytes with nanofillers, such as PEO−$LiClO_4$ with $TiO_2$ nanoparticles (~$1 \times 10^{-5}$ S cm$^{-1}$ at 30 °C),[5] PEO−$LiBF_4$ with $ZrO_2$ (~$1 \times 10^{-7}$ S cm$^{-1}$ at 30 °C),[43] PEO−$LiBF_4$ with $SiO_2$ nanoparticles (~$1 \times 10^{-6}$ S cm$^{-1}$ at 30 °C),[44] the composite electrolyte with YSZ nanowires shows comparable and even higher conductivity.

Interestingly, the improvement in Li-ion conductivity of the composite polymer electrolyte is found to be in connection with oxygen-ion conductivity of the YSZ nanowire. Summarized Li-ion conductivity of the composite polymer electrolytes with YSZ nanowires in terms of concentration of dopant, in comparison to oxygen-ion conductivity (800 °C) of YSZ bulk material, is shown in Figure 4c. It can be seen that at the doping level of 7 mol %, both the Li-ion conductivity for the composite electrolyte and the oxygen-ion conductivity for YSZ approach the maximum value. As is well-known, oxygen vacancy is generated by doping lower valence oxide into $ZrO_2$, which increases with doping level first and then decreases due to the association of oxygen vacancies and cations, resulting in an optimal value of oxygen-ion conductivity at around 7 mol %



DOI: 10.1021/acsnano.6b06797
ACS Nano 2016, 10, 11407−11413

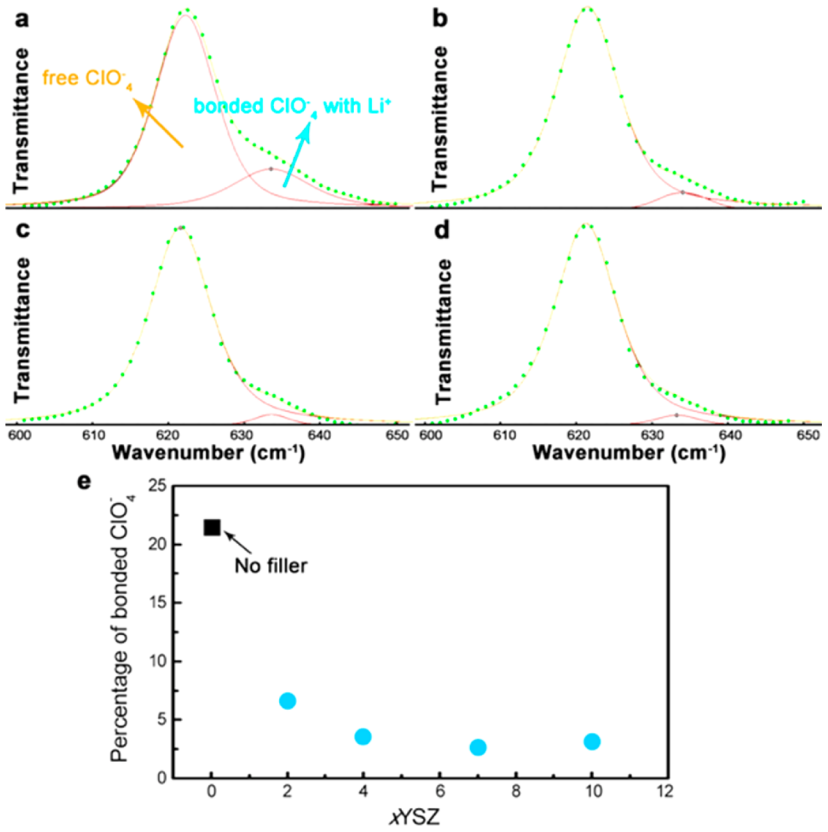


**Figure 5. FTIR spectra for the composite polymer electrolytes filled with YSZ nanowires of various dopants. (a) FTIR spectra for the filler-free electrolyte and the composite polymer electrolytes filled with the (b) 2YSZ, (c) 7YSZ, and (d) 10YSZ nanowires. (e) Plot of the percentage of the peak according to bonded $ClO_4^-$ with $Li^+$ *vs* $Y_2O_3$ doping level.**

doping of $Y_2O_3$ (where YSZ can be fully stabilized into the cubic structure).[37−39,45] Understandably, the free oxygen vacancies with positive charges play a crucial role in the Li-ion conduction in the composite polymer electrolyte.

One explanation for the conductivity improvement by filling the inorganic nanoparticles is the hindrance of the local reorganization of chains in the polymer and then the reduction of the polymer crystallization.[5,46] In present study, Figure S6 shows the thermogravimetric (TG) curves of the composite polymer electrolytes with the YSZ nanowires of various doping levels and the filler-free electrolyte. The first step associated with the cyclization is up to about 250 °C, where weight loss is very small. The second process is up to about 350 °C, showing quite rapid rate of weight loss, which is mainly due to the dehydrogenation of PAN. In the last step, the fragmentation of polymer chains occurs, producing volatile particles leading to the weight loss. The corresponding data are summarized in Figure 4d, displaying the relationship between the ionic conductivity and the dehydrogenation temperature with various Y doping levels. It is found that the variation tendency of conductivity with dopant is inverse to that of dehydrogenation temperature; namely, the conductivity reaches a maximum value while the temperature decreases to the minimum when the 7YSZ nanowire was used. The lower the dehydrogenation temperature, the lower the crystallinity degree of the polymer electrolyte. The surface groups of the ceramic fillers provide physical cross-linking centers for the polymer segments, which allow reduction of the tendency for polymer reorganization. Accordingly, it can be seen that more free oxygen vacancies result in decreased crystallinity degree, promoting the Li-ion conduction.

Another interpretation on the conductivity improvement has been raised by various researchers in terms of Lewis acid−base interaction.[30,47] The additional conducting pathways on the filler surfaces established by the structural modified cations contribute to a highly improvement of Li-ion conductivity. A stronger affinity between positively charged oxygen vacancies on the surfaces of the YSZ nanowires and $ClO_4^-$ can be expected. Figure 5 shows the typical Fourier transform infrared (FTIR) transmittance spectra of the composite polymer electrolytes with the nanowires, together with the data for the filler-free electrolyte. The bands at 623 and 635 $cm^{-1}$ are observed, assigned to the free anions ($ClO_4^-$) that do not interact directly with $Li^+$ and are attributed to the contact ion pairs ($Li^+ClO_4^-$). It reveals that the addition of the YSZ nanowires results in growth of the band at 623 $cm^{-1}$ and the fade of the band at 635 $cm^{-1}$, which indicates that the nanowires help to dissociate $ClO_4^-$ with $Li^+$ and subsequently release more free Li ions.[30,48] Figure 5e also demonstrates that the concentration of the bonded $ClO_4^-$ achieves the minimum value when the dopant is 7 mol %, where the conductivity of the composite electrolyte also reaches the maximum. As a consequence, more free oxygen vacancies on the surfaces of the YSZ nanowires allow more free Li ions, which results in improved conductivity for the composite polymer electrolyte. To confirm increased concentration of free Li ions, the lithium transference number ($t_+$) of the composite polymer electrolytes was measured and calculated with the following equation:[49]



DOI: 10.1021/acsnano.6b06797
ACS Nano 2016, 10, 11407−11413

$$t_+ = \frac{I_{ss}(\Delta V - I_0 R_0)}{I_0(\Delta V - I_{ss}R_{ss})} \quad (2)$$

where $I_0$ and $I_{ss}$ are the initial and steady-state currents, $\Delta V$ is the potential applied across the cell, and $R_0$ and $R_{ss}$ are the initial and steady-state resistance of the passivation layer. The variation of current with time during polarization for the composite polymer electrolyte with 7YSZ nanowires is shown in Figure S7. Subsequently, $t_+$ for the filler-free electrolyte and the composite polymer electrolyte with nanowires is calculated to be 0.27 and 0.56, respectively, which indicates increased free Li-ion concentration.

## CONCLUSION

In summary, we disclose a simple strategy to fabricate the solid composite polymer electrolyte with the YSZ nanowires, which displays an interesting improvement of ionic conductivity with respect to the concentration of free oxygen vacancies in the nanowires. The YSZ nanowires with various $Y_2O_3$ dopants and diameters were successfully prepared by electrospinning. Reduction of cystallinity of the polymer was observed to increase the conductivity of the composite electrolyte. Furthermore, it is proposed that more free oxygen vacancies with positive charge on the surfaces of the nanowires could release more free $Li^+$ ions from the association with $ClO_4^-$ anions. The results reveal that the composite polymer electrolyte filled with the YSZ nanowires of 7 mol % of $Y_2O_3$ shows the maximum concentration of free $Li^+$ ions and accordingly achieves the highest conductivity of $1.07 \times 10^{-5}$ S $cm^{-1}$ at 30 °C. Improved electrochemical stability for the composite polymer electrolyte by addition the nanowires is also observed. The present work pinpoints the high importance of one-dimensional oxygen-ion conducting materials in the application of all-solid-state LIBs.

## METHODS

**Synthesis of the YSZ Nanowires and Nanoparticles.** $ZrOCl_2 \cdot 8H_2O$ (>99.9%) and $Y(NO_3)_3 \cdot 6H_2O$ (>99.9%) of various corresponding molar mass were dissolved in a mixture of deionized water and ethanol or whole ethanol solvent. An appropriate amount of PVP ($M_w$ = 130 000) was subsequently added. A transparent solution with a concentration of 8 wt % PVP was obtained by vigorous stirring. For the electrospinning procedure, the precursor solution was loaded into a capillary with a stainless steel needle. A high voltage of 15 kV was applied by dipping a charged silver thread into the precursor solution. The as-spun fibers were subsequently calcined at 600 °C for 2 h in air at a heating rate of 5 °C $min^{-1}$.

For comparison with the nanowires, 7 mol % of yttria-doped zirconia nanoparticles wasprepared by a sol–gel synthesis using starting materials of $ZrOCl_2 \cdot 8H_2O$ and $Y(NO_3)_3 \cdot 6H_2O$. A transparent viscous gel was obtained by stirring these materials together in ethanol at 90 °C. The dry gel was calcined in the temperature range of 700 °C for 3 h in air.

**Synthesis of the YSZ Nanowire-Filled PAN–$LiClO_4$ Solid Composite Polymer Electrolyte.** YSZ nanowires (15 wt %, total weight of PAN and $LiClO_4$) were added in the DMF solution that contained PAN and $LiClO_4$. The mixture was mechanically stirred at 80 °C for 5 h and then cast with a doctor blade onto a glass plate. Finally, the solid composite polymer electrolytes were dried in high vacuum at 80 °C for 48 h to completely remove the DMF solvent. They were then transferred into an argon-filled glovebox ($O_2$ and $H_2O$ at sub-ppm value, typically <0.6 ppm) and heated at 80 °C for at least 48 h before measurement to completely remove the solvent and moisture. All of the samples, including the filler-free electrolyte and the composite electrolyte with nanowires, were prepared following the same procedures and drying temperature and time.

**Characterization.** TG analyses (STA 449, Netzsch) were conducted to determine the thermal evolution during heating of the polymer electrolytes under simulated air atmosphere (20 vol % of $O_2$ in Ar, 99.99% pure gases from Airgas). XRD (PANalytical X'Pert diffractometer) was used for phase identification using Cu K$\alpha$ radiation of 0.15406 nm. The morphologies of samples were examined by SEM (FEI Nova NanoSEM 450) and TEM (FEI Tecnai G2 F20 X-TWIN microscope). XPS (PHI VersaProbe scanning XPS microprobe) waas carried out on YSZ nanowire powers. FTIR transmittance spectra were taken on a Bruker Vertex 70 FTIR spectrometer. The dried composite polymer electrolyte membrane was sandwiched between two stainless steel (SS) electrodes for conductivity measurements. The electrical conductivity investigated using AC impedance spectroscopies was recorded by a Biologic VSP potentiostat over the frequency range of 0.10 Hz to 1 MHz. Using lithium as a counter and reference electrode, linear sweep voltammetry was performed between −0.5 and +6.0 V (*vs* $Li^+/Li$) on a SS working electrode, at a scanning rate of 1.0 mV $s^{-1}$. All the assemblies were carried out in a dry glovebox filled with argon.

## ASSOCIATED CONTENT

### Supporting Information

The Supporting Information is available free of charge on the ACS Publications website at DOI: 10.1021/acsnano.6b06797.

Detailed description of the experimental procedures, TEM, TG, and XPS characterization of the YSZ nanowires, and supplementary electrochemical data (PDF)

## AUTHOR INFORMATION


### Corresponding Author

*E-mail: yicui@stanford.edu.

### ORCID

Wei Liu: 0000-0002-6206-8321


### Author Contributions

W.L. and Y.C. conceived the experiment and carried out data analysis. W.L. performed materials fabrication and characterization. D.L., N.L., J.S., and G.Z. assisted in experimental work. W.L. and Y.C. wrote the paper. All the authors discussed the results on the manuscript.

### Notes

The authors declare no competing financial interest.

## ACKNOWLEDGMENTS

This work was supported by Samsung Electronics.

## REFERENCES


(1) Bouchet, R.; Maria, S.; Meziane, R.; Aboulaich, A.; Lienafa, L.; Bonnet, J. P.; Phan, T. N. T.; Bertin, D.; Gigmes, D.; Devaux, D.; et al. Single-Ion BAB Triblock Copolymers as Highly Efficient Electrolytes for Lithium-Metal Batteries. *Nat. Mater.* **2013**, *12*, 452–457.

(2) Aricò, A. S.; Bruce, P.; Scrosati, B.; Tarascon, J. M.; Van Schalkwijk, W. Nanostructured Materials for Advanced Energy Conversion and Storage Devices. *Nat. Mater.* **2005**, *4*, 366–377.

(3) Thangadurai, V.; Narayanan, S.; Pinzaru, D. Garnet-Type Solid-State Fast Li Ion Conductors for Li Batteries: Critical Review. *Chem. Soc. Rev.* **2014**, *43*, 4714–4727.

(4) Zheng, G.; Lee, S. W.; Liang, Z.; Lee, H.-W.; Yan, K.; Yao, H.; Wang, H.; Li, W.; Chu, S.; Cui, Y. Interconnected Hollow Carbon Nanospheres for Stable Lithium Metal Anodes. *Nat. Nanotechnol.* **2014**, *9*, 618–623.

(5) Croce, F.; Appetecchi, G. B.; Persi, L.; Scrosati, B. Nanocomposite Polymer Electrolytes for Lithium Batteries. *Nature* **1998**, *394*, 456–458.




DOI: 10.1021/acsnano.6b06797
*ACS Nano* 2016, 10, 11407–11413

(6) Tarascon, J. M.; Armand, M. Issues and Challenges Facing Rechargeable Lithium Batteries. *Nature* **2001**, *414*, 359−367.
(7) Yang, Y.; Zheng, G.; Cui, Y. Nanostructured Sulfur Cathodes. *Chem. Soc. Rev.* **2013**, *42*, 3018−3032.
(8) Busche, M. R.; Drossel, T.; Leichtweiss, T.; Weber, D. A.; Falk, M.; Schneider, M.; Reich, M.-L.; Sommer, H.; Adelhelm, P.; Janek, J. Dynamic Formation of a Solid-Liquid Electrolyte Interphase and Its Consequences for Hybrid-Battery Concepts. *Nat. Chem.* **2016**, *8*, 426−434.
(9) Ding, Y.; Yu, G. A Bio-Inspired, Heavy-Metal-Free, Dual-Electrolyte Liquid Battery towards Sustainable Energy Storage. *Angew. Chem.* **2016**, *128*, 4850−4854.
(10) Ding, Y.; Zhao, Y.; Li, Y.; Goodenough, J. B.; Yu, G. A High-Performance All-Metallocene-Based, Non-Aqueous Redox Flow Battery. *Energy Environ. Sci.* **2016**, DOI: 10.1039/C6EE02057G.
(11) Murugan, R.; Thangadurai, V.; Weppner, W. Fast Lithium Ion Conduction in Garnet-Type $Li_7La_3Zr_2O_{12}$. *Angew. Chem., Int. Ed.* **2007**, *46*, 7778−7781.
(12) Shimonishi, Y.; Zhang, T.; Imanishi, N.; Im, D.; Lee, D. J.; Hirano, A.; Takeda, Y.; Yamamoto, O.; Sammes, N. A Study on Lithium/Air Secondary Batteries-Stability of the NASICON-Type Lithium Ion Conducting Solid Electrolyte in Alkaline Aqueous Solutions. *J. Power Sources* **2011**, *196*, 5128−5132.
(13) Stramare, S.; Thangadurai, V.; Weppner, W. Lithium Lanthanum Titanates: a Review. *Chem. Mater.* **2003**, *15*, 3974−3990.
(14) Kamaya, N.; Homma, K.; Yamakawa, Y.; Hirayama, M.; Kanno, R.; Yonemura, M.; Kamiyama, T.; Kato, Y.; Hama, S.; Kawamoto, K.; Mitsui, A. A Lithium Superionic Conductor. *Nat. Mater.* **2011**, *10*, 682−686.
(15) Mizuno, F.; Hayashi, A.; Tadanaga, K.; Tatsumisago, M. New, Highly Ion-Conductive Crystals Precipitated from $Li_2S$−$P_2S_5$ Glasses. *Adv. Mater.* **2005**, *17*, 918−921.
(16) Agrawal, R. C.; Pandey, G. P. Solid Polymer Electrolytes: Materials Designing and All-Solid-State Battery Applications: an Overview. *J. Phys. D: Appl. Phys.* **2008**, *41*, 223001.
(17) Denoyel, R.; Armand, M.; Fergus, J. W. Ceramic and Polymeric Solid Electrolytes for Lithium-Ion Batteries. *J. Power Sources* **2010**, *195*, 4554−4569.
(18) Gowneni, S.; Ramanjaneyulu, K.; Basak, P. Polymer-Nanocomposite Brush-like Architectures as an All-Solid Electrolyte Matrix. *ACS Nano* **2014**, *8*, 11409−11424.
(19) Liu, W.; Liu, N.; Sun, J.; Hsu, P. C.; Li, Y.; Lee, H. W.; Cui, Y. onic Conductivity Enhancement of Polymer Electrolytes with Ceramic Nanowire Fillers. *Nano Lett.* **2015**, *15*, 2740−2745.
(20) Croce, F.; Persi, L.; Ronci, F.; Scrosati, B. Nanocomposite Polymer Electrolytes and Their Impact on the Lithium Battery Technology. *Solid State Ionics* **2000**, *135*, 47−52.
(21) Min, H. S.; Ko, J. M.; Kim, D. W. Preparation and Characterization of Porous Polyacrylonitrile Membranes for Lithium-Ion Polymer Batteries. *J. Power Sources* **2003**, *119*, 469−472.
(22) Stephan, A. M.; Nahm, K. S. Review on Composite Polymer Electrolytes for Lithium Batteries. *Polymer* **2006**, *47*, 5952−5964.
(23) Qian, X.; Gu, N.; Cheng, Z.; Yang, X.; Wang, E.; Dong, S. Impedance Study of $(PEO)_{10}LiClO_4$−$Al_2O_3$ Composite Polymer Electrolyte with Blocking Electrodes. *Electrochim. Acta* **2001**, *46*, 1829−1836.
(24) Fu, K.; Gong, Y.; Dai, J.; Gong, A.; Han, X.; Yao, Y.; Wang, C.; Wang, Y.; Chen, Y.; Yan, C.; Li, Y.; Wachsman, E. D.; Hu, L. Flexible, Solid-State, Ion-Conducting Membrane with 3D Garnet Nanofiber Networks for Lithium Batteries. *Proc. Natl. Acad. Sci. U. S. A.* **2016**, *113*, 7094−7099.
(25) Wang, Y. J.; Pan, Yi; Kim, D. Conductivity Studies on Ceramic $Li_{1.3}Al_{0.3}Ti_{1.7}(PO_4)_3$-Filled PEO-Based Solid Composite Polymer Electrolytes. *J. Power Sources* **2006**, *159*, 690−701.
(26) Balazs, A. C.; Emrick, T.; Russell, T. P. Nanoparticle Polymer Composites: Where Two Small Worlds Meet. *Science* **2006**, *314*, 1107−1110.
(27) Lin, C. W.; Hung, C. L.; Venkateswarlu, M.; Hwang, B. J. Influence of $TiO_2$ Nano-Particles on the Transport Properties of Composite Polymer Electrolyte for Lithium-Ion Batteries. *J. Power Sources* **2005**, *146*, 397−401.
(28) Fu, K. K.; Gong, Y.; Dai, J.; Gong, A.; Han, X.; Yao, Y.; Wang, C.; Wang, Y.; Chen, Y.; Yan, C.; Li, Y.; Wachsman, E. D.; Hu, L. Flexible, Solid-State, Ion-Conducting Membrane with 3D Garnet Nanofiber Networks for Lithium Batteries. *Proc. Natl. Acad. Sci. U. S. A.* **2016**, *113*, 7094−7099.
(29) Marcinek, M.; Bac, A.; Lipka, P.; Zalewska, A.; Zukowska, G.; Borkowska, R.; Wieczorek, W. Effect of Filler Surface Group on Ionic Interactions in PEG-$LiClO_4$-$Al_2O_3$ Composite Polyether Electrolytes. *J. Phys. Chem. B* **2000**, *104*, 11088−11093.
(30) Wang, Z. X.; Huang, X. J.; Chen, L. Q. Understanding of Effects of Nano-$Al_2O_3$ Particles on Ionic Conductivity of Composite Polymer Electrolytes. *Electrochem. Solid-State Lett.* **2003**, *6*, E40−E44.
(31) Xi, J. Y.; Tang, X. Z. Nanocomposite Polymer Electrolyte Based on Poly (ethylene oxide) and Solid Super Acid for Lithium Polymer Battery. *Chem. Phys. Lett.* **2004**, *393*, 271−276.
(32) Chu, P. P.; Reddy, M. J. $Sm_2O_3$ Composite PEO Solid Polymer Electrolyte. *J. Power Sources* **2003**, *115*, 288−294.
(33) Liu, Y.; Lee, J. Y.; Hong, L. In Situ Preparation of Poly (ethylene Oxide)−$SiO_2$ Composite Polymer Electrolytes. *J. Power Sources* **2004**, *129*, 303−311.
(34) Steele, B. C. H.; Heinzel, A. Materials for Fuel-Cell Technologies. *Nature* **2001**, *414*, 345−352.
(35) Kharton, V. V.; Marques, F. M. B.; Atkinson, A. Transport Properties of Solid Oxide Electrolyte Ceramics: a Brief Review. *Solid State Ionics* **2004**, *174*, 135−149.
(36) Atkinson, A.; Ramos, T. M. G. M. Chemically-Induced Stresses in Ceramic Oxygen Ion-Conducting Membranes. *Solid State Ionics* **2000**, *129*, 259−269.
(37) Goodenough, J. B. Oxide-Ion Electrolytes. *Annu. Rev. Mater. Res.* **2003**, *33*, 91−128.
(38) Yashima, M.; Ohtake, K.; Kakihana, M.; Arashi, H.; Yoshimura, M. Determination of Tetragonal-Cubic Phase Boundary of $Zr_{1-X}R_XO_{2-X2}$ (R= Nd, Sm, Y, Er and Yb) By Raman Scattering. *J. Phys. Chem. Solids* **1996**, *57*, 17−24.
(39) Ochrombel, R.; Schneider, J.; Hildmann, B.; Saruhan, B. Thermal Expansion of EB-PVD Yttria Stabilized Zirconia. *J. Eur. Ceram. Soc.* **2010**, *30*, 2491−2496.
(40) Avnir, D. Organic Chemistry within Ceramic Matrixes: Doped Sol-Gel Materials. *Acc. Chem. Res.* **1995**, *28*, 328−334.
(41) Roy, S.; Ghose, J. Synthesis of Stable Nanocrystalline Cubic Zirconia. *Mater. Res. Bull.* **2000**, *35*, 1195−1203.
(42) Garvie, R. C. Stabilization of the Tetragonal Structure in Zirconia Microcrystals. *J. Phys. Chem.* **1978**, *82*, 218−224.
(43) Croce, F.; Settimi, L.; Scrosati, B. Superacid $ZrO_2$-Added, Composite Polymer Electrolytes with Improved Transport Properties. *Electrochem. Commun.* **2006**, *8*, 364−368.
(44) Liu, Y.; Lee, J. Y.; Hong, L. In Situ Preparation of Poly (ethylene oxide)−$SiO_2$ Composite Polymer Electrolytes. *J. Power Sources* **2004**, *129*, 303−311.
(45) Yamamoto, O. Solid Oxide Fuel Cells: Fundamental Aspects and Prospects. *Electrochim. Acta* **2000**, *45*, 2423−2435.
(46) Nan, C. W.; Fan, L. Z.; Lin, Y. H.; Cai, Q. Enhanced Ionic Conductivity of Polymer Electrolytes Containing Nanocomposite $SiO_2$ Particles. *Phys. Rev. Lett.* **2003**, *91*, 266104.
(47) Wieczorek, W.; Stevens, J. R.; Florjahczyk, Z. Composite Polyether Based Solid Electrolytes. The Lewis Acid-Base Approach. *Solid State Ionics* **1996**, *85*, 67−72.
(48) Chen-Yang, Y. W.; Chen, Y. T.; Chen, H. C.; Lin, W. T.; Tsai, C. H. Effect of the Addition of Hydrophobic Clay on the Electrochemical Property of Polyacrylonitrile/$LiClO_4$ Polymer Electrolytes for Lithium Battery. *Polymer* **2009**, *50*, 2856−2862.
(49) Evans, J.; Vincent, C. A.; Bruce, P. G. Electrochemical Measurement of Transference Numbers in Polymer Electrolytes. *Polymer* **1987**, *28*, 2324−2328.



DOI: 10.1021/acsnano.6b06797
*ACS Nano* 2016, 10, 11407−11413